Effects of N,N-dimethyl-N-alkylamine-N-oxides on DOPC bilayers in unilamellar vesicles: Small-angle neutron scattering study

ARTICLE *in* BIOPHYSICS OF STRUCTURE AND MECHANISM · APRIL 2014

Impact Factor: 2.22 · DOI: 10.1007/s00249-014-0954-0 · Source: PubMed

Eur Biophys J (2014) 43:179–189
DOI 10.1007/s00249-014-0954-0

ORIGINAL PAPER

EBSA
Biophysics in Europe

Effects of *N*,*N*-dimethyl-*N*-alkylamine-*N*-oxides on DOPC bilayers in unilamellar vesicles: small-angle neutron scattering study

Michal Belička · Norbert Kučerka · Daniela Uhríková · Akhmed Kh. Islamov · Alexander I. Kuklin · Ferdinand Devínsky · Pavol Balgavý

Received: 18 January 2014 / Revised: 27 February 2014 / Accepted: 10 March 2014 / Published online: 1 April 2014

Abstract Small-angle neutron scattering data were collected from aqueous dispersions of unilamellar vesicles (ULVs) consisting of mixtures of 1,2-dioleoyl-*sn*-glycero-3-phosphatidylcholine and a homologous series of *N*,*N*-dimethyl-*N*-alkylamine-*N*-oxides (C*n*NO, $n = 12$, 14, 16, and 18, where n is the number of carbon atoms in the alkyl chain). A modeling approach was applied to the neutron scattering curves to obtain the bilayer structural parameters. Particularly, the external $^2H_2O/H_2O$ contrast variation technique was carried out on pure dioleoylphosphatidylcholine (DOPC) ULVs to determine the hydrophilic region thickness $D_h = 9.8 \pm 0.6$ Å. Consequently, the hydrocarbon region thickness $2D_C$, the lateral bilayer area per one lipid molecule A, and the number of water molecules located in the hydrophilic region per one lipid molecule N_W were obtained from single-contrast neutron scattering curves using the previously determined D_h. The structural parameters were extracted as functions of r_{CnNO} (the C*n*NO:DOPC molar ratio) and n. The dependences $A(r_{CnNO})$ provided the partial lateral areas of C*n*NOs ($\bar{A}_{CnNO}$) and DOPC ($\bar{A}_{DOPC}$) in bilayers. It was observed that the $\bar{A}_{CnNO}$'s were constant in the investigated interval of r_{CnNO} and for $n = 12$, 14, and 16 equal to 36.6 ± 0.4 Å^2, while $\bar{A}_{C18NO}$ increased to 39.4 ± 0.4 Å^2. The bilayer hydrocarbon region thickness $2D_C$ decreased with intercalation of each C*n*NO. This effect increased with r_{CnNO} and decreased with increasing C*n*NO alkyl chain length. The intercalation of C18NO changed the $2D_C$ only slightly. To quantify the effect of C*n*NO intercalation into DOPC bilayers we fit the $2D_C(r_{CnNO})$ dependences with weighted linear approximations and acquired their slopes Δd.

Keywords Small-angle neutron scattering · Unilamellar vesicles · Lipid bilayer · Dioleoylphosphatidylcholine · *N*,*N*-Dimethyl-*N*-alkylamine-*N*-oxide

Electronic supplementary material The online version of this article (doi:10.1007/s00249-014-0954-0) contains supplementary material, which is available to authorized users.

M. Belička
Department of Nuclear Physics and Biophysics, Faculty of Mathematics, Physics and Informatics, Comenius University, 842 48 Bratislava, Slovakia

M. Belička (✉) · N. Kučerka · D. Uhríková · F. Devínsky · P. Balgavý
Department of Physical Chemistry of Drugs, Faculty of Pharmacy, Comenius University, Odbojárov 10, 832 32 Bratislava, Slovakia
e-mail: belicka.michal@gmail.com; belicka@fpharm.uniba.sk

N. Kučerka
Chalk River Laboratories, Canadian Neutron Beam Center, Chalk River, ON KOJ 1JO, Canada

A. K. Islamov · A. I. Kuklin
Frank Laboratory of Neutron Physics, Joint Institute for Nuclear Research, 141980 Dubna, Moscow Region, Russia

A. K. Islamov · A. I. Kuklin
Laboratory for Advanced Studies of Membrane Proteins, Moscow Institute of Physics and Technology, 141700 Dolgoprudny, Moscow Region, Russia

Introduction

The structure and physical properties of phospholipid bilayers, the fundamental part of cell membranes, are influenced by a wide range of environment conditions such as the structure of the constituent lipid molecules, their electric charge, the temperature, and the presence of ions in the aqueous environment. This further affects the chemical and biological characteristics of the bilayer. A special kind

of influence is presented by amphiphilic molecules. Their amphiphilic character allows them to insert into lipid bilayers and interact with both the hydrophilic and hydrophobic parts of the bilayer. Due to the complexity of the internal structure of even pure lipid bilayers, the final effect of intercalation depends on many factors. As the lipid bilayers of a cell membrane contain many intercalated molecules, detailed knowledge of the intercalation mechanism of amphiphiles and its impact on the lipid bilayer is important for understanding the structure of cell membranes.

N,*N*-Dimethyl-*N*-alkylamine-*N*-oxides (C*n*NO, where *n* is the number of carbon atoms in the alkyl chain) are widely used in different areas of industry (Devínsky 1986) and have been studied extensively over recent decades (Herrmann 1962; Benjamin 1966; Chang et al. 1985; Maeda et al. 2006; Lorenz et al. 2011). A wide variety of biological activities have been discovered for these compounds, including antimicrobial (Devínsky et al. 1990; Balgavý and Devínsky 1996), antiphotosynthetic (Šeršeň et al. 1990, 1992), immunomodulatory (Jahnová et al. 1993), and phytotoxic effects (Murín et al. 1990). They are also used as mild detergents for solubilization, purification, reconstitution, and crystallization of membrane proteins [see Uhríková et al. (2001) for further references]. As amphiphilic molecules with simple structure—a single alkyl chain attached to the hydrophilic group—they draw attention mainly because of their strongly polar N–O bond located in the polar headgroup with high electron density on the oxygen. However, at physiological pH values, the C*n*NO polar headgroup is nonionic because $pK_a \approx 4.95$ (Búcsi et al. 2014).

Due to their amphiphilic character, C*n*NOs easily insert into lipid bilayers. Depending on their alkyl chain length, a hydrophobic mismatch in the hydrophobic region may occur, which is then compensated by a *trans-gauche* isomerization of hydrocarbon chains or by their mutual interdigitation (Šeršeň et al. 1989; Balgavý et al. 1993). This leads not only to structural changes of the bilayer (Dubničková et al. 1997; Uhríková et al. 2001) but also to an alteration of the dynamical state of the hydrocarbon region (Šeršeň et al. 1989; Glover et al. 1999). Importantly, C*n*NOs have been shown to affect the activity of a transmembrane sarcoendoplasmic reticulum calcium transport ATPase (SERCA) calcium pump (Karlovská et al. 2006). Therefore, the ability of C*n*NOs to induce structural changes in lipid bilayers, in addition to the possibility of controlling their ionic character in situ, makes them very useful and interesting components in biomembrane studies.

In the present paper we study the influence of C*n*NOs on phospholipid bilayers formed by dioleoylphosphatidylcholine (DOPC) in unilamellar vesicles (ULVs) using the method of small-angle neutron scattering (SANS). SANS has proved to be very effective in lipid bilayer structure investigations (Uhríková et al. 2001; Kučerka et al. 2004a, b; Klacsová et al. 2011; Heberle et al. 2012). In the present work we apply the three-strip model of lipid bilayers developed previously by Kučerka et al. (2004a, b). It allows us to evaluate the internal structure of bilayers from SANS curves in terms of the hydrophobic region thickness $2D_C$ and the lateral area of a bilayer per one lipid molecule A. We assume zero hydration in the hydrocarbon chain region, while the intercalation of water molecules into the hydrophilic region is taken into account. To estimate the hydrophilic thickness D_h and the corresponding number of water molecules per one lipid molecule, we utilized the contrast variation technique (Kotlarchyk et al. 1985; Sadler et al. 1990; Pedersen et al. 2003; Kučerka et al. 2004a, b). Although there exist models describing the pure lipid bilayer structure in more detail, e.g., the scattering density profile model (Kučerka et al. 2008, 2009), the simple model used in the present study is suitable for describing the internal structure of mixed bilayers without proliferating the number of parameters. The SANS measurements were performed using the homologous series of C*n*NOs for $n = 12$, 14, 16, and 18 incorporated into DOPC bilayers at 25 °C. The C*n*NO:DOPC molar ratio was changing in the interval 0.0–1.3. The evaluated dependences of A and $2D_C$ allow us to determine the structural changes in the DOPC bilayers induced by the intercalation of C*n*NOs depending on their concentration and alkyl chain length.

Materials and methods

Chemicals

Synthetic DOPC was purchased from Avanti Polar Lipids (Alabaster, USA) in powder form. C*n*NOs ($n = 12$, 14, 16, and 18) were prepared from appropriate *N*,*N*-dimethyl-*N*-alkylamines by oxidation with hydrogen peroxide and purified by a procedure described previously by Devínsky et al. (1978). The organic solvents of spectral purity were purchased from Slavus (Bratislava, Slovakia) and redistilled before use. The heavy water (99.96 % D_2O) was obtained from Merck (Darmstadt, Germany), and the rest of the chemicals used for synthesis of C*n*NOs were from Lachema (Brno, Czech Republic).

Sample preparation

Stock methanol–chloroform solutions of DOPC and C*n*NOs were prepared. Their required volumes were transferred into glass tubes to obtain mixtures with molar ratios $r_{CnNO} = n_{CnNO} : n_{DOPC}$ from 0.1 to 1.3 for each n and one reference sample of pure DOPC. The majority of organic

solvents were evaporated from the solutions by a stream of gaseous nitrogen, and remaining traces were removed by an oil vacuum pump (5 h, 7 Pa). The amounts of dried C*n*NO+DOPC mixtures were checked gravimetrically, hydrated with ^2H_2O to obtain dispersions with lipid concentration of 1.0 wt%, and homogenized by hand shaking and vortex mixing. After visual inspection of homogeneity, each dispersion was extruded 51 times through 50-nm-pore polycarbonate filters (Nuclepore, Pleasanton, USA) mounted in a LiposoFast Basic extruder (Avestin, Ottawa, Canada) fit with two gastight Hamilton syringes (Hamilton, Reno, USA) according to MacDonald et al. (1991). An odd number of extrusion steps was chosen to avoid contamination of samples by large and multilamellar vesicles, which do not pass through a filter. All extrusions were carried out at room temperature, at which all the studied bilayers are in fluid phase. After preparation, the samples were sealed with Parafilm M (American National Can, Greenwich, USA) in Eppendorf plastic tubes under N_2 atmosphere, and stored at room temperature. The samples for analysis by the contrast variation technique were prepared from the sample with $r_{CnNO} = 1.0$ in heavy water by adding appropriate amounts of H_2O and ^2H_2O to obtain samples with the required $^2H_2O/H_2O$ contrasts.

SANS measurements

The SANS measurements were performed on the small-angle time-of-flight axially symmetric neutron scattering spectrometer YuMO with a two-detector system at the IBR-2 fast pulsed reactor (Kuklin et al. 2005, 2006) at the Frank Laboratory of Neutron Physics, JINR, Dubna, Russia. The spectrometer is equipped with two circular multiwire proportional ^{3}He detectors. The sample—first detector distance was set to 5.28 m, and the sample—second detector distance to 13.04 m. The samples were held in quartz cells (Hellma, Müllheim, Germany) of 2 mm thickness during measurements. The sample temperature was set and controlled electronically at 25 ± 0.1 °C, and each sample was equilibrated at a given temperature for at least 1 h before collecting data. The scattering data were corrected for background effects, and the normalized coherent scattering intensities were obtained using a vanadium standard scatterer as described by Ostanevich (1988) and Kuklin et al. (2013).

Data evaluation

Examples of the obtained neutron scattering curves are plotted in Fig. 1. The model neutron scattering intensity $I_{\text{model}}(q)$ can be described by the equation

$$I_{\text{model}}(q) = N_{\text{p}} \cdot S(q) \cdot \overline{||F(q)||^2}, \tag{1}$$

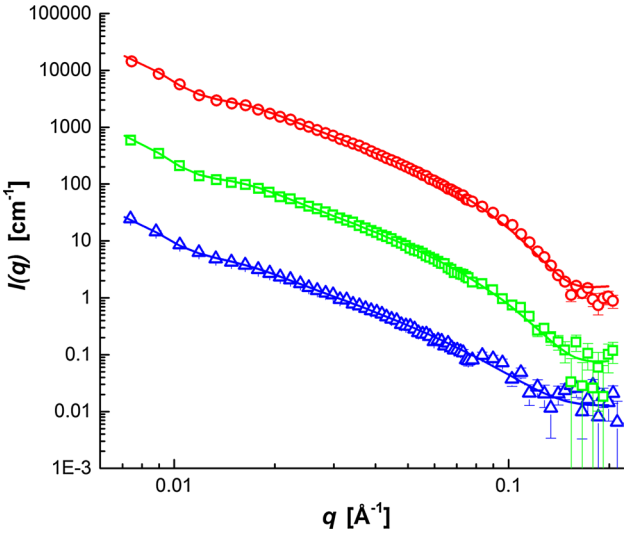

Fig. 1 Contrast variation small-angle scattering curves obtained from pure DOPC ULVs in different $^2H_2O/H_2O$ mixtures: 100 % (*circle*), 70 % (*square*), and 50 % (*triangle*) ^2H_2O. The errors below 0.1 Å^{-1} are smaller than or comparable to *symbols*. *Solid lines* represent the best simultaneous fit of the three-strip model to all three scattering curves with the internal parameter values given in Table 1. The data and fit curves for 100 and 70 % contrasts are shifted in the *vertical direction* for better visualization

where q is the transferred momentum, N_{p} is the number of scattering vesicles in the irradiated volume of a sample, $S(q)$ is the interparticle structure factor of vesicles (dependent on the spatial distribution of vesicles and their size and orientation), and $F(q)$ is the form factor of a single vesicle. $F(q)$, in general, is averaged over all shapes, sizes, and orientations of vesicles in the sample. It has been found experimentally that $S(q) \approx 1.0$ for $q \geq 0.005$, when the solute weight fraction is below 2 wt% (Nawroth et al. 1989; Kiselev et al. 2003).

It was shown previously that the extrusion procedure used in the present study produces unilamellar vesicles (Kučerka et al. 2007) whose radii R' can be described by the Schulz–Flory distribution (Egelhaaf et al. 1996; Hunter and Frisken 1998; Balgavý et al. 2001; Kučerka et al. 2007)

$$f_{\text{Schulz}}(R'; R, \sigma) = \left(\frac{t+1}{R}\right)^{t+1} \frac{R'^t}{\Gamma(t+1)} \exp\left(-\frac{R'(t+1)}{R}\right), \tag{2}$$

where

$$t = \left(\frac{R}{\sigma}\right)^2 - 1, \tag{3}$$

where R is the mean radius, σ its standard deviation, and $\Gamma(x)$ for $x > 0$ is the Gamma function. Extruded vesicles can be considered as hollow spheres formed by a single lipid bilayer with an inner aqueous compartment. We suppose an ideal distribution of C*n*NO inside of the DOPC bilayers

Table 1 Molecular component volumes used in the SANS evaluation

V_{CH}[a]	22.2 Å^3
V_{CH_2}[a]	27.5 Å^3
V_{CH_3}[a]	55.0 Å^3
V_{PC}[a]	325.0 Å^3
V_{NO}[b]	70.2 Å^3
V_W[c]	30.1 Å^3

Molecular volumes obtained by [a] Uhríková et al. (2007) and [b]Bělička et al. (2014), and calculated from data of [c]Lide (2004)

without any lateral phase separations or molar fraction r_{CnNO} variations among the vesicles in each sample. A single ULV can then be described by the three-strip model as a sphere with the shell divided into three distinct regions: two hydrophilic subshells with thickness D_h on the inner and outer sides of the bilayer, containing only hydrophilic components of DOPC and CnNOs and some water molecules, and a purely hydrophobic central subshell with thickness $2D_C$ in between [following the notation of Nagle and Tristram-Nagle (2000), where D_C is the hydrophobic thickness of a single leaflet of the lipid bilayer], which consists only of the hydrocarbon chains of DOPC and CnNOs. The radii of subshell surfaces from the center are as follows: $R_0 = R' - D_C - D_h$, $R_1 = R' - D_C$, $R_2 = R'$, $R_3 = R' + D_C$, and $R_4 = R' + D_C + D_h$. The form factor of a single ULV represented by this three-strip model has the form

$$F(q;R') = \frac{4\pi}{q^3}\sum_{i=1}^{4}\Delta\rho_i(A(q,R_i) - A(q,R_{i-1})), \tag{4}$$

where

$$A(q,R_i) = qR_i\cos(qR_i) - \sin(qR_i) \tag{5}$$

with $\Delta\rho_i = \rho_i - \rho_W$ being the contrast neutron scattering length density (NSLD) of a given subshell against the aqueous phase $\rho_W = b_W/V_W$, where b_W is the neutron scattering length of a single water molecule (averaged in the case of $^2H_2O/H_2O$ mixtures) and V_W is the molecular volume of bulk water. In the case of hydrophilic regions, ρ_h is given by the expression

$$\rho_h = \frac{b_{PC} + r_{CnNO}\cdot b_{NO} + N_W\cdot b_W}{V_{PC} + r_{CnNO}\cdot V_{NO} + N_W\cdot V_W}, \tag{6}$$

where b_{PC} is the neutron scattering length of a phosphatidylcholine headgroup including carbonyls, b_{NO} is the neutron scattering length of a CnNO headgroup, N_W is the number of water molecules located in the bilayer hydrophilic region per one DOPC molecule, V_{PC} is the partial molecular volume of a phosphatidylcholine headgroup, and V_{NO} is the partial molecular volume of a CnNO headgroup. Similarly, the NSLD of the central hydrophobic subshell is

$$\rho_C = \frac{b_C + r_{CnNO}\cdot b_{Cn}}{V_C + r_{CnNO}\cdot V_{Cn}}, \tag{7}$$

where b_C and V_C are the neutron scattering length and partial molecular volume of the DOPC hydrocarbon chains excluding carbonyl carbons, respectively, and b_{Cn} and V_{Cn} are the neutron scattering length and partial molecular volume of the alkyl chain of CnNO, respectively.

It is reasonable to assume D_h and $2D_C$ independent of the vesicle radius. The averaged squared modulus of the form factor in Eq. (1) is then simply obtained by convoluting the squared modulus of a single-vesicle form factor with the Schulz–Flory distribution function

$$\overline{||F(q)||^2} = \int_0^\infty f_{Schulz}(R';R,\sigma)||F(q,R')||^2\,dR'. \tag{8}$$

The neutron scattering lengths and the volumes of molecular components appear in the presented model as internal parameters. The neutron scattering lengths of the components were calculated on the basis of their structure and the data published by Sears (1992). The scattering length of a water molecule at given contrast was calculated as the weighted average of the scattering lengths of ^2H_2O and H_2O molecules based on the contrast composition. The partial molecular volumes of the DOPC and CnNO components were determined previously (Bělička et al. 2014). The partial molecular volume of water in bulk was calculated from its density at 25 °C (Lide 2004). All values of molecular component volumes used in the model are given in Table 1.

The single-vesicle form factor (4) is described by four parameters: R', D_C, D_h, and N_W. However, these are not independent. Considering the known volumetric data, the lateral area per lipid molecule A can be introduced into the vesicle description by the relation

$$\begin{aligned} A &= \frac{V_{PC} + r_{CnNO}\cdot V_{NO} + N_W\cdot V_W}{D_h} \\ &= \frac{2(V_C + r_{CnNO}\cdot V_{Cn})}{2D_C}, \end{aligned} \tag{9}$$

which reduces the number of independent parameters to three, e.g., R', D_C, and D_h. Therefore, the polydisperse system of ULVs is completely described by four parameters within the three-strip model: D_C, D_h, R, and σ.

The resolution function of the spectrometer was also taken into account according to the approach of Pedersen (1993) in the form of convolution of the model neutron scattering intensity (1) with a Gaussian function

$$G(q';q,\Delta q) = \frac{1}{\sqrt{2\pi\,\Delta q^2(q)}}\exp\left(-\frac{(q-q')^2}{2\Delta q^2(q)}\right), \tag{10}$$

where $\Delta q(q)$ is the variance of the transferred momentum value q (Soloviev et al. 2003).

The constant background was also added to the final theoretical neutron scattering intensity $I_{\text{theor}}(q)$ to eliminate the incoherent scattering from the raw data. Hence, the final neutron scattering intensity used in the fitting procedure has the form

$$I_{\text{theor}}(q) = N_{\text{p}} \int G(q'; q, \Delta q) I_{\text{model}}(q')\, \mathrm{d}q' + I_{\text{back}} \qquad (11)$$

and is parameterized by D_{C}, D_{h}, R, σ, N_{p}, and I_{back}.

The measured scattering data were fit with the described theoretical scattering intensity function using the minimization and error analysis library Minuit (CERN Program Library entry D506). The application of the model and the fitting procedure were described more extensively by Kučerka et al. (2004b).

Results and discussion

Examples of the experimental neutron scattering curves are displayed in Figs. 1 and 2. Each scattering curve consists of two data ranges that overlap in the vicinity of $q = 0.07$ Å^{-1} in Fig. 1 or $q = 1.0$ Å^{-1} in Fig. 2. Minor discrepancies among these data are caused by different resolutions arising from different positions of the detectors for given q regions. Their impact on the fitting process is suppressed by the fact that the points with lower resolution (higher Δq) possess higher ΔI and thus lower weight in the reduced $\Delta\chi^2$. The

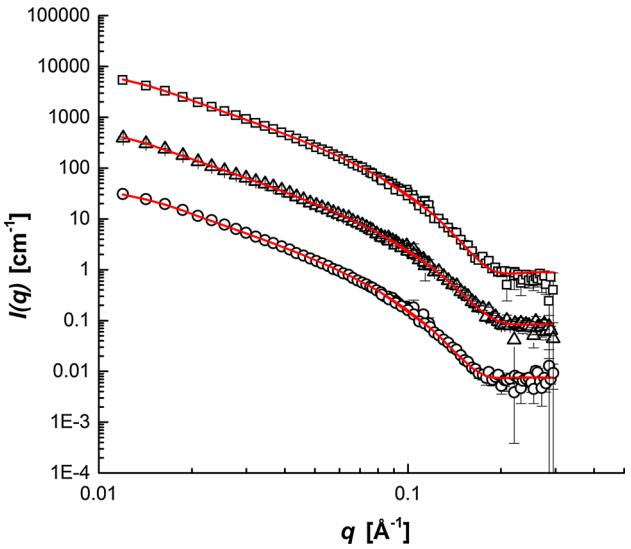

Fig. 2 SANS curves of pure DOPC (*circle*), DOPC+C12NO (*triangle*), and DOPC+C18NO (*square*) ULVs at $r_{C_n\text{NO}} = 1.0$ in ^2H_2O. The *solid lines* are the fits obtained with D_{h} set to 9.83 Å. The data and fits for DOPC+C12NO and DOPC+C18NO are shifted in *vertical direction* for better visualization

application of the described model requires a fixed value of D_{h} for samples measured at a single contrast. Therefore, the measurements were carried out on two kinds of samples. First, SANS on the contrast variation series of pure DOPC in aqueous environment with 100, 70, and 50 % ^2H_2O was measured. This allowed simultaneous fitting of A and D_{h} in addition to other parameters described above. Subsequently, mixtures of DOPC and CnNOs in ^2H_2O with $r_{C_n\text{NO}}$ ranging from 0.1 to 1.3 were measured. No scattering curve displayed a correlation peak indicating intervesicle interactions. Its absence confirms a noninteracting ULV system in each sample, a fundamental assumption of the applied model. As shown by Balgavý et al. (2001) and later by Kučerka et al. (2004a), the region of q influenced by the size distribution of ULVs prepared by the procedure described in "Materials and methods" lies between $q = 0.01$ Å^{-1} and $q = 0.02$ Å^{-1} (i.e., $2\pi/R$, where R is a corresponding mean radius of ULVs). Vesicle size effects in the form of strong minima, characteristic for monodisperse systems, are completely damped by the system polydispersity. Although the affected interval is not large in comparison with the whole measured interval, we fit the ULV size distribution parameters R and σ without constraints whenever possible. At the final step of each data fitting, all parameters were released without any constraints to obtain true unaltered parameter values and their corresponding errors.

Contrast variation measurements

The ULVs are considered as hollow spheres with the same contrasts of inner and outer aqueous compartments in the utilized model. Although during preparation only the contrast of the outer intervesicle environment is changed to the desired composition, the final inner compartment contrast during the measurements was the same as in the intervesicle environment due to the fast interbilayer water diffusion through DOPC bilayers in ULVs [see Huster et al. (1997) and references therein]. The measured curves and the best obtained fits are shown in Fig. 1.

From the best simultaneous fit of three contrast scattering curves we obtained the hydrophilic thickness of pure DOPC bilayers as $D_{\text{h}} = 9.8 \pm 0.6$ Å. To investigate the influence of the model internal parameters, particularly component volumes, on the acquired D_{h} we tested fits with all combinations of extreme values of component volumes of the intervals $V_{\text{mean}} \pm \Delta V$ as they were published by Uhríková et al. (2007) and Belička et al. (2014). We devoted special attention to the DOPC headgroup volume, as it plays a key role in the estimation of the hydrophilic region thickness D_{h}, and further determines the NSLD of hydrophilic region through A (6, 9). Following the same analysis and references as Uhríková et al. (2007), we restricted the variation of the DOPC headgroup volume

to the range of values from $V_{PC} = 319$ Å^3, obtained by Sun et al. (1994) for the dipalmitoylphosphatidylcholine (DPPC) headgroup at 24 °C, to $V_{PC} = 331$ Å^3, obtained by Tristram-Nagle et al. (2002) for the 1,2-dimyristoyl-*sn*-glycero-3-phosphocholine (DMPC) headgroup at 10 °C, and we refit the contrast variation SANS curves for several values of V_{PC} lying between them. We neglected the temperature dependence of V_{PC} due to the small value of its isobaric thermal expansivity coefficient (Uhríková et al. 2007). All values of D_h obtained in the described way lay within the error interval of D_h for $V_{PC} = 325$ Å^3.

To examine the influence of incorporated C*n*NO molecules on the bilayer D_h, we applied the same model with the same component volumes as in the case of contrast variation of pure DOPC ULVs to the contrast variation curves of ULVs consisting of DOPC+C*n*NO mixtures for $n = 12$, 14, and 16 with $r_{CnNO} = 1.0$ (measured on the PAXE spectrometer, LLB Saclay, France; not shown). The homologous series of C*n*NOs were chosen to examine a possible influence of the alkyl chain length of C*n*NO on the resultant D_h of DOPC+C*n*NO ULVs. All three evaluated values of D_h lay within the error margins of D_h belonging to pure DOPC bilayers.

Kučerka et al. (2009) used the scattering length density profile model for simultaneous evaluation of small-angle neutron and X-ray data acquired from ULVs consisting of monounsaturated diacylphosphatidylcholines with different acyl chain lengths at 30 °C. From their results for the bilayer thickness (defined as the distance between the Gibbs dividing surfaces of water) and the hydrocarbon region thickness $2D_C$ (defined by the Gibbs dividing surface of hydrocarbon chains), we calculated $D_h = 9.9 \pm 0.5$ Å for ULVs consisting of pure DOPC as the distance between these two Gibbs surfaces. The same model was applied by Pan et al. (2008) to investigate the temperature dependences of the DOPC bilayer structure parameters in the temperature range of 15–45 °C using diffuse X-ray scattering on oriented stacks and ULVs. The electron density profiles of hydrophilic regions showed no significant differences between the temperature shifts of the phosphate and the glycerol-carbonyl group positions in the investigated temperature interval. This allows one to neglect potential changes in the DOPC headgroup orientation caused by temperature in the given temperature interval. Pabst et al. (2000) reanalyzed neutron diffraction data measured formerly by Büldt et al. (1979) and Zaccai et al. (1979) on aligned DPPC multilayers at low water content (10 and 25 wt%) using the bilayer model, where hydrophilic headgroups and a hydrocarbon region are represented by Gaussians. They obtained a headgroup thickness of $D_h = 9.0 \pm 1.2$ Å, which is in agreement with the value obtained in the present paper ($D_h = 9.8 \pm 0.6$ Å) for $V_{PC} = 325$ Å^3 (see above).

The reviewed results for the headgroup region thickness show good agreement with the value obtained in the current study. They also display differences which might be caused by, in addition to the applied model, the influence of temperature, pressure, chain tilt, and hydration, as also pointed out by Pabst et al. (2000). The fact that our value of D_h lies within the error margins of published results, and the fact that it was obtained at the same environmental conditions as for the rest of the measured samples, lead us to conclude that $D_h = 9.8$ Å represents the headgroup thickness adequately for the applied bilayer model and the resolution of the method used for its investigation. Therefore, during the evaluation of single-contrast scattering curves we set D_h to 9.8 Å and used it as an additional internal parameter.

Single-contrast measurements

The single-contrast scattering curves were fit with D_h fixed to 9.8 Å as explained above. Example fits are shown in Fig. 2. For each mixed DOPC+C*n*NO ULVs the dependences of parameters R, σ, N_W, A, and $2D_C$ as functions of the molar ratio r_{CnNO} were evaluated. The values obtained for DOPC+C12NO are displayed in Figs. 3, 4, and 5. For $n = 14$, 16, and 18 the corresponding dependences had similar character as for C12NO and are shown in the Electronic Supplementary Material (ESM). The values of R and σ could be evaluated only from a limited number of experimental points below 0.02 Å^{-1}. Nevertheless, results appear to show two regions of increased values for R and σ around $r_{CnNO} = 0.3$ and $r_{CnNO} = 1.0$. While the second increase is further suppressed with increasing C*n*NO alkyl chain length and has almost a flat shape for $n = 18$, the increase

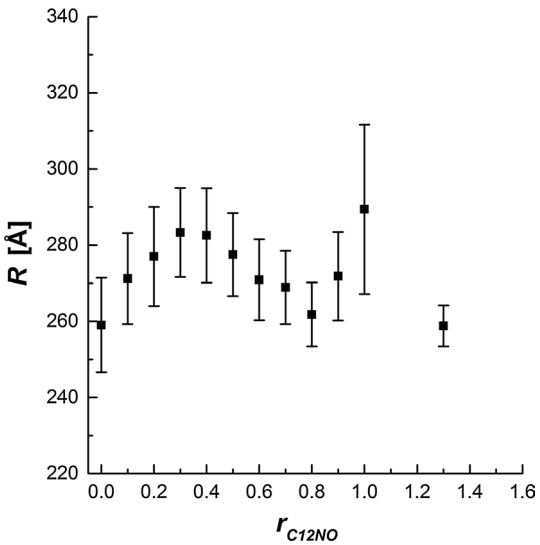

Fig. 3 Mean radius of ULVs consisting of DOPC+C12NO as a function of the molar ratio r_{C12NO}

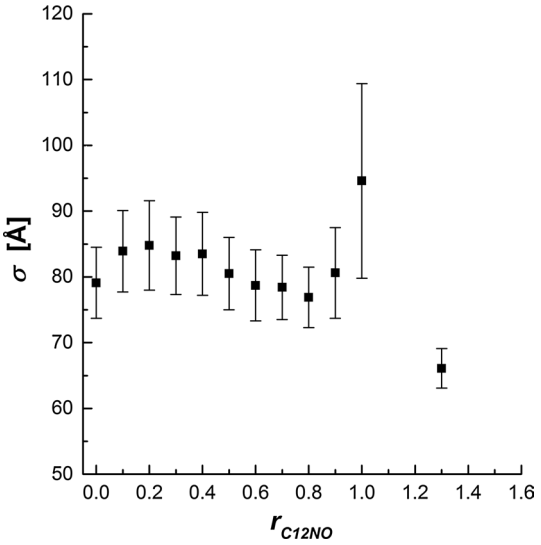

Fig. 4 Standard deviation of the radius of ULVs consisting of DOPC+C12NO as a function of the molar ratio r_{C12NO}

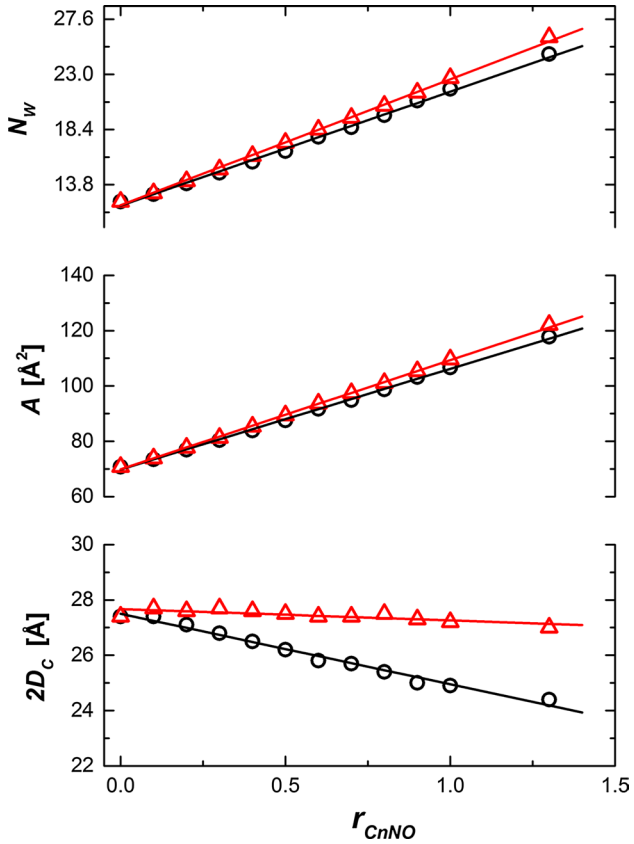

Fig. 5 Number of water molecules located in the hydrophilic region per one lipid molecule N_W, the lateral area of the bilayer per one lipid molecule A, and the hydrocarbon region thickness $2D_C$ of bilayers consisting of DOPC+C12NO (*circle*) and DOPC+C18NO (*triangle*) as a function of the molar ratio r_{CnNO}. *Solid lines* represent weighted linear fits of the data

in the first region persists for all investigated C*n*NOs (see figures in the ESM). The dependences of N_W, A, and $2D_C$ on r_{CnNO} exhibit characters close to linear dependence with different rates of scatter, so their evaluation was carried out by error weighted linear fits (Fig. 5). As N_W is not an independent parameter [see Eq. (9)], further analysis of the DOPC+C*n*NO bilayer structure is mainly concerned with A and $2D_C$.

The single-contrast fit of pure DOPC vesicles in ^2H_2O provided the hydrocarbon region thickness $2D_C = 27.4 \pm 0.1$ Å and the lateral lipid molecule area $A = 70.4 \pm 0.8$ Å^2. Kučerka et al. (2009) described the structure of DOPC bilayers at 30 °C by simultaneous application of a scattering length density profile model to the data acquired from small-angle X-ray scattering and small-angle neutron scattering including the neutron contrast variation technique. From the results of Kučerka et al. (2009) for 30 °C we recalculated, using the lateral area expansivity coefficient $\alpha_A = 0.0029$ K^{-1} and the (hydrocarbon) thickness contractivity coefficient $\alpha_{DC} = 0.0019$ K^{-1} published by Pan et al. (2008), the values $A = 65.9 \pm 1.0$ Å^2 and $2D_C = 29.3 \pm 0.2$ Å corresponding to 25 °C. To resolve the inconsistency between these values and the values obtained in the present work, we refit the single-contrast scattering curve of pure DOPC ULVs in 100 % ^2H_2O with $V_{PC} = 319$ and 331 Å^3 to see the influence of the V_{PC} value on A and D_C. Since the changes were only $\Delta D_C < 0.2$ Å and $\Delta A < 0.4$ Å^2, we focused on the hydrophilic region thickness as a potential source of the discrepancy. Regardless of the value of D_h obtained from the contrast variation technique, we refit the same single-contrast curve with $D_h = 8.0$ and 12.0 Å to see its influence on the investigated parameters. Even with this variation of ±2.0 Å in D_h we observed variations of only $\Delta D_C < 0.6$ Å and $\Delta A < 1.5$ Å^2. This emphasizes the complexity of a model-based approach to data analysis, and suggests the limitations of our more trivial model. We would like to emphasize however that this is not a criticism of simpler models, whose appropriate use is determined by the amount of available experimental data.

The acquired A dependences on r_{CnNO} display increasing character for all C*n*NOs that can be approximated by linear functions in the given range of r_{CnNO} (see Fig. 5 and ESM). The slopes of the A dependences and their fits are not the same for all the studied C*n*NOs though. Whereas A changes with increasing r_{CnNO} similarly for $n = 12$, 14, and 16, in the case of C18NO the A rises more steeply. We evaluated these dependences in terms of the partial molecular areas of DOPC and the C*n*NOs to investigate quantitatively the influence of the C*n*NO alkyl chain length on A. It follows directly from the meaning of A that $n_{DOPC}A = n_{DOPC}A_{DOPC} + n_{CnNO}A_{CnNO}$ and thus

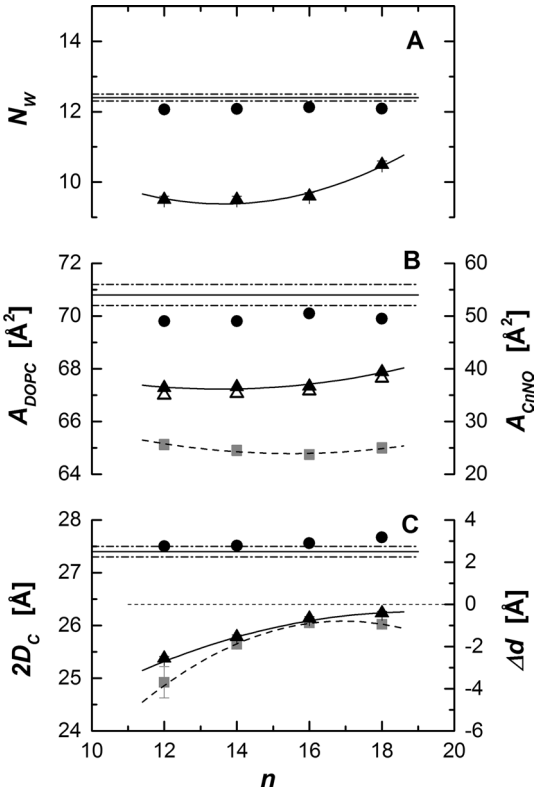

Fig. 6 Results of weighted linear fits of the number of water molecules in the hydrophilic region per one lipid molecule N_W (**a**), the lateral area of the bilayer per one lipid molecule A (**b**), and the hydrocarbon region thickness of the bilayer $2D_C$ (**c**) as functions of r_{CnNO} for $n = 12$, 14, 16, and 18 and the values of A_{CnNO} and Δ_{PP} for corresponding C*n*NOs adopted from Karlovská et al. (2004) (*grey squares*, *full black square*). The *curves* are drawn only to guide the eye. If the *error bars* are not seen, the errors are smaller than the size of *symbols*. **a** The number of water molecules intercalated into the hydrophilic region belonging to one molecule of lipid (*full black circles*) and a C*n*NO molecule (*full black triangles*). The *solid line* represents the number of intercalated water molecules per one lipid molecule in pure DOPC bilayers obtained from the control sample; the *dashed lines* represent its uncertainty. **b** The partial (*full black symbols*) and the apparent (*empty symbols*) areas of DOPC (*circles*) and C*n*NO molecules (*triangles*). The *solid line* represents the apparent lateral area of a lipid molecule in the pure DOPC bilayer obtained from the control sample, and the *dash-dotted lines* its uncertainty. **c** The hydrocarbon region thickness of the DOPC bilayer unaffected by C*n*NO molecules (*full black symbols*) and the slopes of the $2D_C$ dependences on r_{CnNO}'s Δd (*full black triangles*) obtained by weighted linear fits

$A = A_{DOPC} + r_{CnNO}A_{CnNO}$. The linear characters of the studied dependences suggest that A_{DOPC} and A_{CnNO} are constant in the studied r_{CnNO} interval. Keeping A_{DOPC} released during the fitting process and set to its apparent value from the single-contrast fit of pure DOPC ULVs in ^2H_2O, we obtain the partial ($\bar{A}_{DOPC}$, $\bar{A}_{CnNO}$) and the apparent lateral areas (A_{DOPC}, A_{CnNO}) of a lipid molecule and a C*n*NO molecule, respectively. The results are depicted in Fig. 6. The values of $\bar{A}_{C12NO} = 36.4 \pm 0.4$ Å^2, $\bar{A}_{C14NO} = 36.6 \pm 0.4$ Å^2, and $\bar{A}_{C16NO} = 36.7 \pm 0.7$ Å^2 are equal within their uncertainties, whereas there is a significant increase in the case of $\bar{A}_{C18NO} = 39.4 \pm 0.9$ Å^2. The corresponding $\bar{A}_{DOPC}$'s lie in the interval 69.8–70.1 Å^2 for all the C*n*NOs and are equal within their error margins of ±0.2 Å^2. The $\bar{A}_{DOPC}$ values are just slightly lower than $A_{DOPC} = 70.8 \pm 0.4$ Å^2 obtained from the pure DOPC bilayers in the control sample. The A_{CnNO}'s (Table 2) are lower than the corresponding $\bar{A}_{CnNO}$'s but follow the same tendency. From the agreement between $\bar{A}_{DOPC}$ and A_{DOPC}, we conclude that the application of linear approximations was appropriate and the obtained values and trends are correct within the applied model.

Table 2 Partial ($\bar{A}_{CnNO}$, $\bar{A}_{DOPC}$) and apparent (A_{CnNO}) lateral molecular areas of DOPC and C*n*NOs, the slope of the hydrocarbon region thickness as a function of r_{CnNO}, and the number of water molecules in the hydrophilic region corresponding to one C*n*NO molecule, obtained from weighted linear fits for different C*n*NO alkyl chain lengths

n	$\bar{A}_{CnNO}$ (Å^2)	A_{CnNO} (Å^2)	$\bar{A}_{DOPC}$ (Å^2)	Δd (Å)	N_W(C*n*NO)
12	36.4 ± 0.4	35.0 ± 0.2	69.8 ± 0.2	−2.55 ± 0.08	9.5 ± 0.1
14	36.6 ± 0.4	35.3 ± 0.2	69.8 ± 0.2	−1.54 ± 0.09	9.5 ± 0.1
16	36.7 ± 0.4	35.8 ± 0.2	70.1 ± 0.2	−0.66 ± 0.08	9.6 ± 0.1
18	39.4 ± 0.4	38.2 ± 0.2	69.9 ± 0.2	−0.41 ± 0.08	10.5 ± 0.1

Karlovská et al. (2004) investigated the influence of C*n*NO homologs on the structure of lipid bilayers consisting of egg yolk phosphatidylcholine (EYPC) at 20 °C by small-angle X-ray scattering (SAXS) and via the Luzzati (1968) model. As the interpretation of SAXS data by the Luzzati gravimetric model was not possible for fully hydrated bilayer systems in excess of water in their work, Karlovská et al. (2004) investigated EYPC+C*n*NO mixtures at different degrees of low hydration up to 20 mol H_2O/mol EYPC. Due to low hydration, the mixtures formed lamellar phases, in contrast to our samples, which were fully hydrated in water excess and formed ULVs. Based on the Luzzati model of a bilayer lamellar phase, Karlovská et al. (2004) fit the dependences of A on r_{CnNO} for different EYPC+C*n*NO mixed bilayers for different degrees of hydration and obtained A_{CnNO}'s as functions of the system hydration as well as n. The A_{CnNO}'s obtained in the present work and the A_{CnNO}'s from the work of Karlovská et al. (2004) at hydration of 12 mol/mol EYPC are compared in Fig. 6b. There is visible disagreement between their SAXS and our SANS data in the values. A_{CnNO} varies between 35 and 38.2 Å^2 in our SANS results, whereas the SAXS results of Karlovská et al. (2004) vary in the range of 23.7–25.6 Å^2. These discrepancies are most likely caused by the different hydrations. The difference in lipid species should influence the results insignificantly as EYPC possesses the same polar headgroup as DOPC and the average hydrocarbon chain composition of EYPC [C17.8:1.2PC;

for references see Karlovská et al. (2004)] is also roughly the same as the acyl chains of DOPC (C18:1PC). Most importantly, comparison of the A_{CnNO} tendencies in the SANS and the SAXS data shows only a subtle difference for C*n*NOs with shorter alkyl chains, while both sets show similar upward trends with increasing n.

It is of interest to compare our A_{CnNO}'s with the results from C*n*NO micelle studies. Barlow et al. (2000) investigated the structure of C12NO micelles at various concentrations in ^2H_2O at 25 °C by the SANS method. They considered a polydisperse system of micelles consisting of a purely hydrophobic core formed by alkyl chains of C12NOs and a hydrophilic region consisting of the polar headgroups and water molecules filling gaps. The best fit described the C12NO micelles as prolate ellipsoids formed by 103 ± 2 C12NO molecules, with hydrophilic region thickness of 4 Å and outer lateral area per one C12NO molecule equal to $A_{C12NO} = 71$ Å^2. The component volumes of C12NO used by Barlow et al. (2000) were based on the original values published by Benjamin (1966). If we adopt the same component volumes, we can compare their results with others in earlier works. Gorski et al. (1994) measured SANS on micelles formed by C14NO in ^2H_2O at 25 °C. The micellar system was described as monodisperse, consisting of micelles represented by homogeneous spheres without any internal structure and parameterized only by their radius. They obtained a mean micelle radius of 31.7 Å, which corresponds to the aggregation of 276 C14NO molecules with outer lateral area per C14NO molecule of $A_{C14NO} = 45.8$ Å^2. Garamus et al. (1999) also studied a micellar system formed by C12NO in ^2H_2O at 25 °C by SANS, describing it as monodisperse and consisting of micelles with a hydrophobic core according to the ideas of Tanford (1980) and a hydrophilic region similar to that of Barlow et al. (2000). Their results showed prolate ellipsoidal micelles with aggregation number of 78 ± 2 molecules and an outer surface characterized by semiaxes of 46 ± 3 and 20 ± 2 Å, providing an outer lateral molecular area of $A_{C12NO} = 124 \pm 19$ Å^2. Recently, Lorenz et al. (2011) carried out molecular dynamics simulations of nonionic C12NO micelles. The micelles with water were modeled in a 100 × 100 × 100 Å^3 box at $T = 300$ K. After equilibration, the modeled micelle consisted of 68 C12NO molecules and was characterized by an outer radius of 22.7 Å and a hydrophilic region thickness of $D_h = 1.2$ Å. The calculated outer lateral area per C12NO molecule was 94.8 Å^2. Even though the A_{CnNO}'s obtained from SANS on aqueous micellar solutions of C*n*NOs show a wide spread, their values are clearly higher than in the case of C*n*NO molecules intercalated into lipid bilayers. This supports the assumption of a more compact packing of C*n*NOs in lipid bilayers in comparison with micelles.

The intercalation of each studied C*n*NO into the DOPC bilayer reduces the hydrocarbon region thickness $2D_C$. This effect increases with r_{CnNO} and decreases with increasing C*n*NO alkyl chain length (Fig. 5). The dependences of $2D_C$ on r_{CnNO} display tendencies that can be successfully described by linear functions. Hence, we fit them by weighted linear approximations to obtain $2D_C$'s unaffected by intercalation and the corresponding slopes Δd's for different alkyl chain lengths n. The slopes increase almost linearly as n goes from 12 to 16, while there is a change between $n = 16$ and $n = 18$. For $n = 18$, $\Delta d(n = 18)$ is very close to zero. The fits of $2D_C$ values interpolated to $r_{CnNO} = 0.0$ are in good agreement with the value obtained from the control sample of pure DOPC ULVs. The described effect of C*n*NOs on the DOPC bilayer thickness can be explained in terms of "free" volume compensation, in which voids, formed due to a chain length mismatch of C*n*NOs and DOPC below the terminal C*n*NO methyl group, are immediately eliminated by *trans-gauche* isomerizations of acyl chains or by their interdigitation (Devínsky et al. 1990; Balgavý and Devínsky 1996). The longer the C*n*NO incorporated into the DOPC bilayer, the smaller the formed voids, and the smaller the volume of neighboring acyl chains needed to fill them. This idea agrees very well with the observed results, as Δd is almost equal to zero for C18NO, whose alkyl chain length is comparable to the length of DOPC acyl chains. The presented results were also compared with the results from SAXS acquired by Karlovská et al. (2004). From the SAXS measurements on EYPC+C*n*NO lamellar phases, the phosphate–phosphate distance across the bilayer d_{PP} was obtained by inverse Fourier transformation for each sample. Simply, the value of d_{PP} gives the distance between two maxima in a bilayer electron density profile corresponding to polar headgroup positions in the bilayer. From their averaged values obtained from samples hydrated above 15 mol H_2O/mol EYPC, and thus where d_{PP} did not change significantly with hydration because of water incorporation only into interlamellar space, the dependences $d_{PP}(r_{CnNO})$ were evaluated. Their linear fits yield slopes Δ_{PP} which are displayed with our SANS results for Δd in Fig. 6. Our SANS results for Δd are in good agreement with the SAXS results for Δ_{PP} obtained by Karlovská et al. (2004). Δd increases as $\Delta d = 19.83 - 1.53n + 0.06n^2$ (quadratic fit in Ångströms).

Conclusions

We carried out SANS measurements on DOPC+C*n*NO ULVs in aqueous solution. Applying the three-strip model for the ULV description, we investigated the influence of intercalation of C*n*NOs into DOPC bilayers in fluid phase on their structure with increasing r_{CnNO} and alkyl chain length n. The contrast variation technique allowed us to determine the hydrophilic region thickness of DOPC bilayers as $D_h = 9.8 \pm 0.6$ Å, which is in accordance with previously

published values for phosphatidylcholines. Subsequently, we set D_h equal to the obtained value and treated it as another fixed internal parameter. This provided the possibility to evaluate the single-contrast neutron scattering curves from the DOPC+C*n*NO ULVs with the three-strip model. Among other dependences, we acquired the lateral bilayer area per one lipid molecule A and the hydrocarbon region thickness $2D_C$ as functions of r_{CnNO} and n. By evaluation of the dependences $A(r_{CnNO})$ we obtained the partial $\bar{A}_{CnNO}$ and the apparent A_{CnNO} lateral areas of C*n*NOs in the bilayer. The A_{CnNO} 's were lower than the $\bar{A}_{CnNO}$'s by less than 0.5 Å^2 and both displayed the same tendency as functions of n, being nearly constant for $n = 12$, 14, and 16 but increasing by less than 3 Å^2 for $n = 18$. We compared our results for $\bar{A}_{CnNO}$ with the results for A_{CnNO} obtained by the SAXS method applied on EYPC+C*n*NO mixtures at low hydration, where we found a disagreement in numerical values due to the different hydrations of the compared systems, but good agreement in the tendencies of $\bar{A}_{CnNO}$ (SANS) and A_{CnNO} as functions of n. The dependences of $2D_C$ on r_{CnNO} showed a decreasing character for all investigated n. It was found that the slope of decrease Δd increased with n, and that for C18NO was almost zero. This was also compared with the SAXS results, showing excellent agreement with our SANS results.

Acknowledgments This work was supported by JINR project 04-4-1069-2009/2014, by the VEGA 1/0159/11 and 1/1224/12 grants, and by the APVV-0212-10 grant.

References

Balgavý P, Devínsky F (1996) Cut-off effects in biological activities of surfactants. Adv Colloid Int Sci 66:23–63. doi:10.1016/0001-8686(96)00295-3

Balgavý P, Uhríková D, Gallová J, Lohner K, Degovics G (1993) Interaction of tertiary amine anesthetics with phosphatidylcholine bilayers. In: Laggner P, Glatter O (eds) Trends in colloid interface science VII. Steinkopff, Germany, pp 184–185. doi:10.1007/BFb0118503

Balgavý P, Kučerka N, Gordeliy VI, Cherezov VG (2001) Evaluation of small-angle neutron scattering curves of unilamellar phosphatidylcholine liposomes using a multishell model of bilayer neutron scattering length density. Acta Phys Slovaca 51:53–68

Barlow DJ, Lawrence MJ, Zuberi T, Zuberi S, Heenan RK (2000) Small-angle neutron-scattering studies on the nature of the incorporation of polar oils into aggregates of *N*,*N*-dimethyldodecylamine-*N*-oxide. Langmuir 16:10398–10403. doi:10.1021/la0002233

Belička M, Klacsová M, Karlovská J, Westh P, Devínsky F, Balgavý P (2014) Molecular and component volumes of *N*,*N*-dimethyl-*N*-alkylamine-*N*-oxides in DOPC bilayers. Chem Phys Lipids 180:1–6. doi:10.1016/j.chemphyslip.2014.02.007

Benjamin L (1966) Partial molal volume changes during micellization and solution of nonionic surfactants and perfluorocarboxylates using a magnetic density balance. J Phys Chem 70:3790–3797. doi:10.1021/j100884a006

Búcsi A, Karlovská J, Chovan M, Devínsky F, Uhríková D (2014) Determination of pK_a of *N*-alkyl-*N*,*N*-dimethylamine-*N*-oxides using ^{1}H NMR and ^{13}C NMR spectroscopy. Chem Pap 68:842–846. doi: 10.2478/s11696-013-0517-3

Büldt G, Gally HU, Seelig J, Zaccai G (1979) Neutron diffraction studies on phosphatidylcholine model membranes: I. Head group conformation. J Mol Biol 134:673–691. doi:10.1016/0022-2836(79)90479-0

Chang DL, Rosano HL, Woodward AE (1985) Carbon-13 NMR study of the effects of pH on dodecyldimethylamine oxide solutions. Langmuir 1:669–672. doi:10.1021/la00066a006

Devínsky F (1986) Amine oxides. XVII. Non-aromatic amine oxides: Their use in organic synthesis and industry. Acta Fac Pharm Univ Comen 40:63–83

Devínsky F, Lacko I, Nagy A, Krasnec L (1978) Amine oxides. I. Synthesis, ^{1}H-NMR, and infrared spectra of 4-alkylmorpholine-*N*-oxides. Chem Zvesti: Chem Pap 32:106–115

Devínsky F, Kopecká-Leitmanová A, Šeršeň F, Balgavý P (1990) Cut-off effect in antimicrobial activity and in membrane perturbation efficiency of the homologous series of *N*,*N*-dimethylalkylamine oxides. J Pharm Pharmacol 42:790–794. doi:10.1111/j.2042-7158.1990.tb07022.x

Dubničková M, Kiselev M, Kutuzov S, Devínsky F, Gordeliy V, Balgavý P (1997) Effect of *N*-lauryl-*N*, *N*-dimethylamine-*N*-oxide on dimyristoyl phosphatidylcholine bilayer thickness: a small-angle neutron scattering study. Gen Physiol Biophys 16:175

Egelhaaf SU, Wehrli E, Müller M, Adrian M, Schurtenberger P (1996) Determination of the size distribution of lecithin liposomes: a comparative study using freeze fracture, cryoelectron microscopy and dynamic light scattering. J Microsc 184:214–228. doi:10.1046/j.1365-2818.1996.1280687.x

Garamus V, Kameyama K, Kakehashi R, Maeda H (1999) Neutron scattering and electrophoresis of dodecyldimethylamine oxide micelles. Colloid Polym Sci 277:868–874. doi:10.1007/s003960050463

Glover RE, Smith RR, Jones MV, Jackson SK, Rowlands CC (1999) An EPR investigation of surfactant action on bacterial membranes. FEMS Microbiol Lett 177:57–62. doi:10.1111/j.1574-6968.1999.tb13713.x

Gorski N, Gradzielski M, Hoffmann H (1994) Mixtures of nonionic and ionic surfactants. The effect of counterion binding in mixtures of tetradecyldimethylamine oxide and tetradecyltrimethylammonium bromide. Langmuir 10:2594–2603. doi:10.1021/la00020a018

Heberle FA, Pan J, Standaert RF, Drazba P, Kučerka N, Katsaras J (2012) Model-based approaches for the determination of lipid bilayer structure from small-angle neutron and X-ray scattering data. Eur Biophys J 41:875–890. doi:10.1007/s00249-012-0817-5

Herrmann KW (1962) Non-ionic—cationic micellar properties of dimethylamine oxide. J Phys Chem 66:295–300. doi:10.1021/j100808a025

Hunter DG, Frisken BJ (1998) Effect of extrusion pressure and lipid properties on the size and polydispersity of lipid vesicles. Biophys J 74:2996–3002. doi:10.1016/S0006-3495(98)78006-3

Huster D, Jin AJ, Arnold K, Gawrisch K (1997) Water permeability of polyunsaturated lipid membranes measured by ^{17}O NMR. Biophys J 73:855–864. doi:10.1016/S0006-3495(97)78118-9

Jahnová E, Ferenčík M, Nyulassy Š, Devínsky F, Lacko I (1993) Amphiphilic detergents inhibit production of IgG and IgM by human peripheral blood mononuclear cells. Immunol Lett 39:71–75. doi:10.1016/0165-2478(93)90166-Y

Karlovská J, Lohner K, Degovics G, Lacko I, Devínsky F, Balgavý P (2004) Effects of non-ionic surfactants *N*-alkyl-*N*,*N*-dimethylamine-*N*-oxides on the structure of a phospholipid bilayer: small-angle X-ray diffraction study. Chem Phys Lipids 129:31–41. doi:10.1016/j.chemphyslip.2003.11.003

Karlovská J, Uhríková D, Kučerka N, Teixeira J, Devínsky F, Lacko I, Balgavý P (2006) Influence of *N*-dodecyl-*N*,*N*-dimethylamine *N*-oxide on the activity of sarcoplasmic reticulum Ca^{2+}-transporting ATPase reconstituted into diacylphosphatidylcholine vesicles:

effects of bilayer physical parameters. Biophys Chem 119:69–77. doi:10.1016/j.bpc.2005.09.007
Kiselev MA, Lombardo D, Kisselev AM, Lesieur P, Aksenov VL (2003) Structure factor of dimyristoylphosphatidylcholine unilamellar vesicles: small-angle X-ray scattering study. Poverhnost 11:20–24
Klacsová M, Bulacu M, Kučerka N, Uhríková D, Teixeira J, Marrink SJ, Balgavý P (2011) The effect of aliphatic alcohols on fluid bilayers in unilamellar DOPC vesicles—a small-angle neutron scattering and molecular dynamics study. Biochim Biophys Acta 1808:2136–2146. doi:10.1016/j.bbamem.2011.04.010
Kotlarchyk M, Huang JS, Chen SH (1985) Structure of AOT reversed micelles determined by small-angle neutron scattering. J Phys Chem 89:4382–4386. doi:10.1021/j100266a046
Kučerka N, Kiselev MA, Balgavý P (2004a) Determination of bilayer thickness and lipid surface area in unilamellar dimyristoylphosphatidylcholine vesicles from small-angle neutron scattering curves: a comparison of evaluation methods. Eur Biophys J 33:328–334. doi:10.1007/s00249-003-0349-0
Kučerka N, Nagle JF, Feller SE, Balgavý P (2004b) Models to analyze small-angle neutron scattering from unilamellar lipid vesicles. Phys Rev E 69:051903. doi:10.1103/PhysRevE.69.051903
Kučerka N, Pencer J, Sachs JN, Nagle JF, Katsaras J (2007) Curvature effect on the structure of phospholipid bilayers. Langmuir 23:1292–1299. doi:10.1021/la062455t
Kučerka N, Nagle JF, Sachs JN, Feller SE, Pencer J, Jackson A, Katsaras J (2008) Lipid bilayer structure determined by the simultaneous analysis of neutron and X-ray scattering data. Biophys J 95:2356–2367. doi:10.1529/biophysj.108.132662
Kučerka N, Gallová J, Uhríková D, Balgavý P, Bulacu M, Marrink S-J, Katsaras J (2009) Areas of monounsaturated diacylphosphatidylcholines. Biophys J 97:1926–1932. doi:10.1016/j.bpj.2009.06.050
Kuklin AI, Islamov AK, Gordeliy VI (2005) Two-detector system for small-angle neutron scattering instrument. Neutron News 16:16–18. doi:10.1080/10448630500454361
Kuklin AI, Islamov AK, Kovalev YS, Utrobin PK, Gordeliy VI (2006) Optimization two-detector system small-angle neutron spectrometer YuMO for nanoobject investigation. J Surf Invest X-Ray Synchrotron Neutron Tech 6:74–83
Kuklin AI, Kovalev YC, Ivankov AI, Soloviev DV, Rogachev AV, Soloviev AG, Utrobin PK, Gordeliy VI (2013) Some specific features of experiment realization at SANS spectrometer at IBR-2. In: Communication P14-2013-46 of the Joint Institute for Nuclear Research, Dubna. http://www1.jinr.ru/Preprints/2013/046(P14-2013-46).pdf
Lide DR (2004) CRC handbook of chemistry and physics 2004–2005: a ready-reference book of chemical and physical data. CRC Press, Boca Raton
Lorenz CD, Hsieh C-M, Dreiss CA, Lawrence MJ (2011) Molecular dynamics simulations of the interfacial and structural properties of dimethyldodecylamine-*N*-oxide micelles. Langmuir 27:546–553. doi:10.1021/la1031416
Luzzati V (1968) X-ray diffraction studies of lipid-water systems. In: Chapman D (ed) Biological membranes. Academic, London, pp 71–123
MacDonald RC, MacDonald RI, Menco BPM, Takeshita K, Subbarao NK, Hu L (1991) Small-volume extrusion apparatus for preparation of large, unilamellar vesicles. Biochim Biophys Acta 1061:297–303. doi:10.1016/0005-2736(91)90295-J
Maeda H, Tanaka S, Ono Y, Miyahara M, Kawasaki H, Nemoto N, Almgren M (2006) Reversible micelle-vesicle conversion of oleyldimethylamine oxide by pH changes. J Phys Chem B 110:12451–12458. doi:10.1021/jp056967c
Murín A, Devínsky F, Koleková A, Lacko I (1990) Relation between chemical structure and biological activity of *N*-alkyl dimethylaminoxides series and some other related components. Biologia (Bratislava) 45:521–531
Nagle JF, Tristram-Nagle S (2000) Structure of lipid bilayers. Biochim Biophys Acta 1469:159–195. doi:10.1016/S0304-4157(00)00016-2
Nawroth T, Conrad H, Dose K (1989) Neutron small angle scattering of liposomes in the presence of detergents. Phys B 156–157:477–480. doi:10.1016/0921-4526(89)90708-4
Ostanevich YM (1988) Time-of-flight small-angle scattering spectrometers on pulsed neutron sources. Macromol Symp 15:91–103. doi:10.1002/masy.19880150107
Pabst G, Rappolt M, Amenitsch H, Laggner P (2000) Structural information from multilamellar liposomes at full hydration: full q-range fitting with high quality X-ray data. Phys Rev E 62:4000–4009. doi:10.1103/PhysRevE.62.4000
Pan J, Tristram-Nagle S, Kučerka N, Nagle JF (2008) Temperature dependence of structure, bending rigidity, and bilayer interactions of dioleoylphosphatidylcholine bilayers. Biophys J 94:117–124. doi:10.1529/biophysj.107.115691
Pedersen JS (1993) Resolution effects and analysis of small-angle neutron scattering data. J Phys IV Fr 3:C8–C491. doi:10.1051/jp4:19938102
Pedersen JS, Svaneborg C, Almdal K, Hamley IW, Young RN (2003) A small-angle neutron and X-ray contrast variation scattering study of the structure of block copolymer micelles: corona shape and excluded volume interactions. Macromolecules 36:416–433. doi:10.1021/ma0204913
Sadler DM, Reiss-Husson F, Rivas E (1990) Thickness measurements of single walled dimyristoyl phosphatidylcholine vesicles by neutron scattering. Chem Phys Lipids 52:41–48. doi:10.1016/0009-3084(90)90005-C
Sears VF (1992) Neutron scattering lengths and cross sections. Neutron News 3:26–37. doi:10.1080/10448639208218770
Šeršeň F, Leitmanová A, Devínsky F, Lacko I, Balgavỳ P (1989) A spin label study of perturbation effects of *N*-(1-methyldodecyl)-*N*,*N*,*N*-trimethylammonium bromide and *N*-(1-methyldodecyl)-*N*,*N*-dimethylamine oxide on model membranes prepared from *Escherichia coli*-isolated lipids. Gen Physiol Biophys 8:133–156
Šeršeň F, Balgavý P, Devínsky F (1990) Electron spin resonance study of chloroplast photosynthetic activity in the presence of amphiphilic amines. Gen Physiol Biophys 9:625–633
Šeršeň F, Gabunia G, Krejčířová E, Kráľová K (1992) The relationship between lipophilicity of *N*-alkyl-*N*,*N*-dimethylamine oxides and their effects on the thylakoid membranes of chloroplasts. Photosynthetica 26:205–212
Soloviev AG, Litvinenko EI, Ososkov GA, Islamov AK, Kuklin AI (2003) Application of wavelet analysis to data treatment for small-angle neutron scattering. Nucl Instrum Methods Phys Res Sect A 502:500–502. doi:10.1016/S0168-9002(03)00481-9
Sun W-J, Suter RM, Knewtson MA, Worthington CR, Tristram-Nagle S, Zhang R, Nagle JF (1994) Order and disorder in fully hydrated unoriented bilayers of gel-phase dipalmitoylphosphatidylcholine. Phys Rev E 49:4665–4676. doi:10.1103/PhysRevE.49.4665
Tanford C (1980) The hydrophobic effect, 2nd edn. Wiley, New York
Tristram-Nagle S, Liu Y, Legleiter J, Nagle JF (2002) Structure of gel phase DMPC determined by X-ray diffraction. Biophys J 83:3324–3335. doi:10.1016/S0006-3495(02)75333-2
Uhríková D, Kučerka N, Islamov A, Gordeliy V, Balgavý P (2001) Small-angle neutron scattering study of *N*-dodecyl-*N*,*N*-dimethylamine *N*-oxide induced solubilization of dioleoylphosphatidylcholine bilayers in liposomes. Gen Physiol Biophys 20:183–189
Uhríková D, Rybár P, Hianik T, Balgavý P (2007) Component volumes of unsaturated phosphatidylcholines in fluid bilayers: a densitometric study. Chem Phys Lipids 145:97–105. doi:10.1016/j.chemphyslip.2006.11.004
Zaccai G, Büldt G, Seelig A, Seelig J (1979) Neutron diffraction studies on phosphatidylcholine model membranes: II. Chain conformation and segmental disorder. J Mol Biol 134:693–706. doi:10.1016/0022-2836(79)90480-7